

# Nonmesonic Weak Decay Spectra and Three-Nucleon Emission

Claudio De Conti<sup>a</sup> Airton Deppman<sup>b</sup> Franjo Krmpotić<sup>c</sup>

<sup>a</sup>*Campus Experimental de Itapeva, Universidade Estadual Paulista, 18409-010, Itapeva, SP, Brazil*

<sup>b</sup>*Instituto de Física, Universidade de São Paulo, São Paulo, Brasil*

<sup>c</sup>*Instituto de Física La Plata, CONICET, 1900 La Plata, Argentina, and Facultad de Ciencias Astronómicas y Geofísicas, Universidad Nacional de La Plata, 1900 La Plata, Argentina.*

## Abstract

We have evaluated the nonmesonic weak decay spectra within the independent-particle shell-model, and compared them with the recent measurements of: i) the single and double coincidence nucleon spectra in  $^{12}_{\Lambda}\text{C}$  performed at KEK, and ii) proton kinetic energy spectra in  $^5_{\Lambda}\text{He}$ ,  $^7_{\Lambda}\text{Li}$ ,  $^9_{\Lambda}\text{Be}$ ,  $^{11}_{\Lambda}\text{B}$ ,  $^{12}_{\Lambda}\text{C}$ ,  $^{13}_{\Lambda}\text{C}$ ,  $^{15}_{\Lambda}\text{N}$  and  $^{16}_{\Lambda}\text{O}$  done by FINUDA. Based on this comparison we argue that the extraction from the data of the three-body  $\Lambda NN \rightarrow nNN$  induced decay rate, as done in these works, could be questionable.

*Key words:*  $\Lambda$ -hypernuclei, nonmesonic weak decay, two-nucleon induced decay  
*PACS:* 21.80.+a, 25.80.Pw

## 1. Introduction

The weak decay rate of a  $\Lambda$  hypernucleus can be cast as [1]

$$\Gamma_W = \Gamma_M + \Gamma_{NM}, \quad (1)$$

where  $\Gamma_M$  is decay rate for the mesonic (M) decay  $\Lambda \rightarrow \pi N$ , and  $\Gamma_{NM}$  is the rate for the nonmesonic (NM) decay, which can be induced either by one bound nucleon (1N),  $\Gamma_1(\Lambda N \rightarrow nN)$ , or by two bound nucleons (2N),  $\Gamma_2(\Lambda NN \rightarrow nNN)$ , where  $N = p, n$  *i.e.*,

$$\Gamma_{NM} = \Gamma_1 + \Gamma_2; \quad \Gamma_1 = \Gamma_p + \Gamma_n, \quad \Gamma_2 = \Gamma_{nn} + \Gamma_{np} + \Gamma_{pp}. \quad (2)$$

<sup>1</sup> Corresponding author: Franjo Krmpotić, e-mail address: krmpotic@fisica.unlp.edu.ar

While the  $M$  and  $1N$ -NM decays have been seen experimentally in the pioneering measurement performed more than 50 years ago by Schneps, Fry, and Swami [2], the experimental observation of the  $2N$ -NM decay, which was predicted by Alberico *et al.* [3] in 1991 (see also Ref. [4]), has been reported only quite recently at KEK [5], and at FINUDA [6]. Both groups announced a branching ratio  $\Gamma_2/\Gamma_{NM} \sim 25 - 30 \%$ . The first group obtained this result from the single and double coincidence nucleon spectra in  ${}_{\Lambda}^{12}\text{C}$ , and the second one from proton kinetic energy spectra in  ${}_{\Lambda}^5\text{He}$ ,  ${}_{\Lambda}^7\text{Li}$ ,  ${}_{\Lambda}^9\text{Be}$ ,  ${}_{\Lambda}^{11}\text{B}$ ,  ${}_{\Lambda}^{12}\text{C}$ ,  ${}_{\Lambda}^{13}\text{C}$ ,  ${}_{\Lambda}^{15}\text{N}$  and  ${}_{\Lambda}^{16}\text{O}$ . A branching ratio for the  $2N$ -NM decaying channel of such a magnitude is consistent with the prediction made by Bauer and Garbarino [7], but it is very large in comparison with the upper limit  $\Gamma_2/\Gamma_W \leq 0.097$  (95% CL), established previously from the single-particle proton and neutron kinetic energy spectra in  ${}_{\Lambda}^4\text{He}$  at BNL [8]. In this experiment it was also found that the effect of the final state interactions (FSIs) is relatively small, its upper limit being  $\Gamma_{NM}^{FSI}/\Gamma_W \leq 0.11$  (95% CL).<sup>2</sup>

Quite recently, Bauer and Garbarino [10] have obtained good agreement with KEK data [5], considering both the one- and the two-nucleon induced decays in the framework of the Fermi Gas Model (FGM). These authors have also analyzed the proton  ${}_{\Lambda}^{12}\text{C}$  spectrum measured at FINUDA [6], but no theoretical study of the remaining spectra has been done so far. The aim of the present work is twofold. First, we confront the results of the independent particle shell model (IPSM) for the  $1N$ -NM decay with the above mentioned experiments. Second, based on this comparison we expose our doubts about the reliability of the procedures followed in these works to extract the ratio  $\Gamma_2/\Gamma_{NM}$  from data.

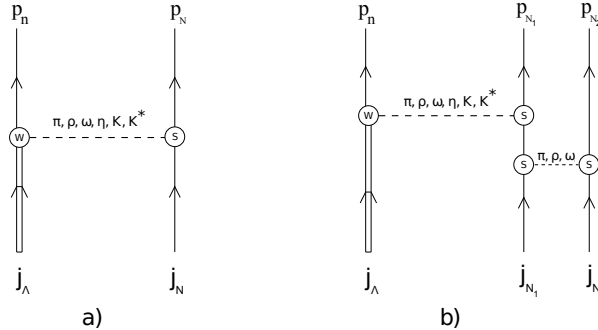


Fig. 1. Schematic representation of a) one-nucleon, and b) two-nucleon induced decays in  $\Lambda$ -hypernuclei when described by the interplay of weak ( $W$ ) and strong ( $S$ ) interactions through the exchanges of nonstrange-mesons  $\pi, \rho, \omega$ , and  $\eta$ , and strange-mesons  $K$ , and  $K^*$ .

The schematic representation of the two channels, when the decay dynamics is accounted for by the one meson-exchange (OME), is shown in Fig. 1. This is the most frequently used model for handling the NM-decay, and includes the exchanges of nonstrange-mesons  $\pi, \rho, \omega$ , and  $\eta$ , and strange-mesons  $K$ , and  $K^*$ . It is based on the original idea of Yukawa that the  $NN$  interaction at long distance is due to the one-pion-exchange (OPE), the dominant role being played by the exchange of pion and kaon mesons.

<sup>2</sup> In fact, the  ${}_{\Lambda}^4\text{He}$  spectra are accounted for reasonably well theoretically by considering the  $1N$ -NM decay mode only [9].

The OPE potential was verified quantitatively by the Nijmegen partial wave analysis of the NN scattering in the elastic region [11]. *i.e.*, at distances larger than the minimal de Broglie wavelength  $1/\sqrt{m_\pi M} \sim 0.5$  fm corresponding to the pion production threshold. The verification of other meson exchanges is less straightforward, and the uncertainties in the baryon-baryon-meson (BBM) coupling constants could be quite sizeable since they are not constrained by experiments. To derive them in the strong sector (S vertices in Fig. 1) the  $SU(3)_f$  (flavor) symmetry is utilized. In the weak sector (W vertex in Fig. 1) the BBM parity-violating couplings are obtained from the  $SU(6)_W$  (weak) symmetry, while the parity conserving ones are derived from a pole model with only baryon pole resonances [12].

The uncertainties regarding the BBM coupling constants are amplified still further by the short-range correlations (SRCs) between the emitted nucleons  $nN$ , and  $nNN$ . Parreño, and Ramos have shown that they can diminish the value of  $\Gamma_1$  by more than a factor of two [13]. Nothing has been said so far regarding the effect of the SRCs on the  $2N$ -NM decay. The theoretical scene becomes still more complex when effects of quark degrees of freedom [14,15], the  $2\pi$ -exchanges [16–18], and the axial-vector  $a_1$ -meson exchange [18] are considered.

To derive the ratio  $\Gamma_2/\Gamma_{NM}$  from data, both KEK [5] and FINUDA [6] teams have included the FSIs in their analysis. The first group has used them to gauge their experimental data on single and double coincidence nucleon spectra in  $^{12}\text{C}$ . For this purpose they have used the Intranuclear Cascade (INC) code, which was developed by Ramos *et al.* [19] to follow the fate of nucleons produced by the primary  $1N$ -NM and  $2N$ -NM decays. On the other hand, the FINUDA's group [6], in their analysis of proton kinetic energy spectra in several hypernuclei, have assumed that the basic role of the FSIs is to shift the transition strength from high energy to low energy, without substantially modifying the total number of protons.

The above mentioned experiments, together with several others performed during the last decade [20–28], represent very important advances in our knowledge about the NM decay. Explicitly, they are: 1) new high quality measurements of single-nucleon spectra  $S_N(E_N)$ , as a function of one-nucleon energy  $E_N$ , and 2) first measurements of the two-particle-coincidence spectra, as a function of: i) the sum of kinetic energies  $E_n + E_N \equiv E_{nN}$ ,  $S_N(E_{nN})$ , ii) the opening angle  $\theta_{nN}$ ,  $S_N(\cos \theta_{nN})$ , and iii) the center of mass (c.m.) momentum  $P_{nN} = |\mathbf{P}_{nN}|$ ,  $S_N(P_{nN})$  with  $\mathbf{P}_{nN} = \mathbf{p}_n + \mathbf{p}_N$ . On the theoretical side this implies a new challenge for nuclear models which now have to explain, not only the  $1N$ - and  $2N$ -NM decay rates, but also the shapes and magnitudes of all these spectra, testing in this way both the kinematics and the dynamics.

The measured spectra are obtained by counting the numbers of emitted nucleons  $\Delta N_N$  within the energy bin  $\Delta E = 10$  MeV, or the angular bin  $\Delta \cos \theta = 0.05$  always corrected by the detection efficiency. Here we take advantage of the fact that in the KEK experiments [5,25,29]  $\Delta N_N$  are normalized to the number of NM processes  $N_{NM}$ , while for the FINUDA proton spectra [6,30] we have at our disposal also the number of produced hypernuclei  $N_W$ . Therefore, we can exploit the following relationships

$$\frac{\Delta N_N}{N_{NM}} = \frac{\Delta \Gamma_N^{exp}}{\Gamma_{NM}}, \quad \frac{\Delta N_N}{N_W} = \frac{\Delta \Gamma_N^{exp}}{\Gamma_W}, \quad (3)$$

where  $\Delta \Gamma_N^{exp}$  is the emission rate of protons within the experimentally fixed bin. Thus,

$$\frac{N_N}{N_{NM}} = \frac{\Gamma_N^{exp}}{\Gamma_{NM}}, \quad \frac{N_N}{N_W} = \frac{\Gamma_N^{exp}}{\Gamma_W}, \quad (4)$$

where  $N_N = \sum_{i=1}^m \Delta N_N$  is the total number of NM events decaying to the mode  $N$ , and  $\Gamma_N^{exp} = \sum_{i=1}^m \Delta \Gamma_N^{exp}$ , is the corresponding decay rate;  $m$  is the number of bins. We note that the last relation in (4) agrees with Eq. (13) in Ref. [8], and that  $\Gamma_N^{exp}$  accounts for both the  $1N$ -NM and  $2N$ -NM decays as well as for the FSIs.

The correspondence between theory and data is

$$\Delta \Gamma_N^{th} \iff \Delta \Gamma_N^{exp} = \Gamma_{NM} \frac{\Delta N_N}{N_{NM}} \Big|_{KEK} = \Gamma_W \frac{\Delta N_N}{N_W} \Big|_{FINUDA}. \quad (5)$$

For  $^{12}\text{C}$  is  $\Gamma_{NM} = 0.95 \pm 0.04$  [5], and as it was pointed out in Ref. [28]

$$\Gamma_W(A) = (0.990 \pm 0.094) + (0.018 \pm 0.010) A, \quad (6)$$

for all measured hypernuclei in the mass range  $A = 4 - 12$ . The theoretical decay widths are  $\Delta \Gamma_N^{th} = S_N(E_N) \Delta E$ , *etc.* Below we briefly sketch the corresponding expressions for spectral densities  $S_N$  within the IPSM.

## 2. IPSM for the $1N$ -NM decay

Within the IPSM [9,31–40]: i) the initial hypernuclear state is taken as a hyperon  $\Lambda$  in single-particle state  $j_\Lambda = 1s_{1/2}$  weakly coupled to an  $(A - 1)$  nuclear core of spin  $J_C$ , i.e.,  $|J_I\rangle \equiv |(J_C j_\Lambda) J_I\rangle$ , ii) the nucleon ( $N = p, n$ ) inducing the decay is in the single-particle state  $j_N$  ( $j \equiv nlj$ ), iii) the final residual nucleus states are:  $|J_F\rangle \equiv |(J_C j_N^{-1}) J_F\rangle$ , iv) the liberated energy is

$$\Delta_N^j = \Delta + \varepsilon_\Lambda + \varepsilon_N^j, \quad (7)$$

where  $\varepsilon$ 's are single-particle energies, and  $\Delta = M_\Lambda - M$ , and  $\mathbf{v}$ ) the c.m. momenta, and relative momenta of the emitted particles are:

$$P_{nN} = \sqrt{(A-2)(2M\Delta_N^j - p_n^2 - p_N^2)}, \quad p_{nN} = \sqrt{M\Delta_N^j - \frac{A}{4(A-2)} P_{nN}^2}. \quad (8)$$

It follows that the  $1N$ -NM decay rate reads

$$\Gamma_N = \sum_j \Gamma_N^j; \quad \Gamma_N^j = \int \mathcal{I}_N^j(p_{nN}, P_{nN}) d\Omega_{nN}, \quad (9)$$

where  $d\Omega_{nN}$  is the phase space factor, which depends on the spectra that one is interested in, and

$$\mathcal{I}_N^j(p_{nN}, P_{nN}) = \sum_{J=|j-1/2|}^{J=j+1/2} F_{NJ}^j \sum_L \mathcal{T}_{NJL}^j(p_{nN}) \mathcal{O}_L^2(P_{nN}). \quad (10)$$

The information on nuclear structure is contained in the spectroscopic factor

$$F_{NJ}^j = \hat{J}_I^{-2} \sum_{J_F} |\langle J_I | (a_{j_N}^\dagger a_{j_\Lambda}^\dagger)_J | J_F \rangle|^2, \quad (11)$$

where  $\hat{J} = \sqrt{2J+1}$ . The values for  $J_I$ , and  $J_C$  are taken from experimental data and for hypernuclei of interest here are listed in Tables I of Ref. [37]. The resulting factors  $F_{NJ}^j$  are presented in Tables II of the same paper.

The kinematics are enclosed in: i) the phase space factor  $d\Omega_{nN}$ , and ii) the overlap

$$\mathcal{O}_L(P_{nN}) = \int R^2 dR j_L(P_{nN} R) R_{0L}(b/\sqrt{2}, R), \quad (12)$$

between the c.m. radial wave functions  $R_{0L}$  of the bound particle and  $j_L$  of the outgoing particle, where  $b$  is the harmonic oscillator size parameter.

The decay dynamics is contained in

$$\mathcal{T}_{NJL}^j(p_{nN}) = \sum_{S\Lambda T} |\mathcal{M}(p_{nN}; lL\lambda S J T; j_\Lambda j_N J \mathbf{t}_{\Lambda N})|^2, \quad (13)$$

where  $\lambda = \mathbf{l} + \mathbf{L}$ , with  $\mathbf{l}$  and  $\mathbf{L}$  being, respectively, relative and c.m. angular momenta,  $T \equiv \{TM_T, M_T = m_{t_\Lambda} + m_{t_N}\}$ , and  $\mathbf{t}_{\Lambda N} \equiv \{t_\Lambda = 1/2, m_{t_\Lambda} = -1/2, t_N = 1/2, m_{t_N}\}$ , with  $m_{t_p} = 1/2$ , and  $m_{t_n} = -1/2$ , where we have assumed that the  $\Lambda N \rightarrow nN$  interaction occurs with the isospin change  $\Delta T = 1/2$ . Moreover

$$\begin{aligned} \mathcal{M}(p_{nN}; lL\lambda S J T; j_\Lambda j_N J \mathbf{t}_{\Lambda N}) &= \frac{1}{\sqrt{2}} [1 - (-)^{l+S+T}] \\ &\times (lL\lambda S J T | V(p_{nN}) | j_\Lambda j_N J \mathbf{t}_{\Lambda N}), \end{aligned} \quad (14)$$

where (and henceforth) the ket  $| \rangle$ , unlike  $| \rangle$ , indicates that the state is not antisymmetrized, and  $V(p_{nN})$  is the transition potential.

To find the kinetic energy  $E_N$  and opening angle  $\theta_{nN}$  spectra it is convenient to express the single-particle transition rate as

$$\Gamma_N = (A-2) \frac{8M^3}{\pi} \sum_{j_N} \int_{-1}^{+1} d \cos \theta_{nN} \int_0^{\tilde{E}_{j_N}} dE_N \sqrt{\frac{E_N}{E'_N}} E_n \mathcal{I}_{j_N}(p_{nN}, P_{nN}), \quad (15)$$

with

$$E'_N = (A-2)(A-1)\Delta_{j_N} - E_N[(A-1)^2 - \cos^2 \theta_{nN}], \quad (16)$$

$$E_n = \left[ \sqrt{E'_N} - \sqrt{E_N} \cos \theta_{nN} \right]^2 (A-1)^{-2}, \quad (17)$$

and

$$\tilde{E}_{j_N} = \frac{A-1}{A} \Delta_{j_N}. \quad (18)$$

Throughout the integration one has to enforce the condition  $E'_N > E_N \cos^2 \theta_{nN}$ . It might be worth noticing that, while  $E'_N$  does not have a direct physical meaning,  $E_n$  is

the energy of the neutron that is the decay-partner of the nucleon  $N$  with energy  $E_N$ . The corresponding spectra read

$$S_N(E_N) = \frac{d\Gamma_N}{dE_N} = (A-2) \frac{8M^3}{\pi} \sum_{j_N} \int_{-1}^{+1} d\cos\theta_{nN} \sqrt{\frac{E_N}{E'_N}} E_n \mathcal{I}_{j_N}(p_{nN}, P_{nN}), \quad (19)$$

and

$$S_N(\cos\theta_{nN}) = \frac{d\Gamma_N}{d\cos\theta_{nN}} = (A-2) \frac{8M^3}{\pi} \sum_{j_N} \int_0^{\tilde{E}_{j_N}} dE_N \sqrt{\frac{E_N}{E'_N}} E_n \mathcal{I}_{j_N}(p_{nN}, P_{nN}). \quad (20)$$

As one-proton (one-neutron) induced decay prompts the emission of an  $np$  ( $nn$ ) pair the total neutron kinetic energy spectrum is:

$$S_{nt}(E_n) = \frac{d\Gamma_{nt}}{dE_n} \equiv S_p(E_n) + 2S_n(E_n), \quad (21)$$

where  $\Gamma_{nt} = \Gamma_p + 2\Gamma_n$  is the total neutron transition rate.

Similarly, we get

$$S_N(E_{nN}) = \frac{4M^3}{\pi} \sqrt{A(A-2)^3} \sum_{j_N} \sqrt{(\Delta_{j_N} - E_{nN})(E_{nN} - \tilde{\Delta}_{j_N})} \mathcal{I}_{j_N}^j(p_{nN}, P_{nN}), \quad (22)$$

for the kinetic energy sum  $E_{nN} = E_n + E_N$ , and

$$S_N(P_{nN}) = \frac{2M}{\pi} \sqrt{\frac{A}{A-2}} \sum_{j_N} P_{nN}^2 \sqrt{P_{j_N}^2 - P_{nN}^2} \mathcal{I}_{j_N}(p_{nN}, P_{nN}), \quad (23)$$

for the c.m. momentum  $P_{nN}$  spectra, with

$$\tilde{\Delta}_{j_N} = \Delta_{j_N} \frac{A-2}{A}, \quad \text{and} \quad P_{j_N} = 2\sqrt{\frac{A-2}{A}} M \Delta_{j_N} \quad (24)$$

being, respectively, the maximum values of  $E_{nN}$ , and  $P_{nN}$  for each  $j_N$ .

The outline of the numerical calculation is the following: a) The transition potential for the emission of the  $nN$  pair,  $V(p_{nN})$  in Eq. (14), is described by two OME models with the weak coupling constants from Ref. [12,13], namely: M1) only the  $\pi + K$  exchange is considered, and M2) the full  $\pi + K + \eta + \rho + \omega + K^*$  is taken into account, b) The initial and final SRCs, as well as the finite nucleon size effects are included in the same way as in our previous works [9,31–38], and c) The parameter  $b$  in Eq. (12) is evaluated as in Ref. [32], *i.e.*,  $b = 1/\sqrt{\hbar\omega M_N}$ , with  $\hbar\omega = 45A^{-1/3} - 25A^{-2/3}$  MeV.

### 3. KEK Experiment

In Figs. 2, 3, and 4 we compare the KEK [5,29] experimental data with the IPSM calculations. As seen from Fig. 2 the calculated proton and neutron kinetic energy spectra agree fairly well with data for  $E_N > 40$  MeV, and specially when the  $\pi + K$  potential is used, in spite of not considering the FSIs. This is not the case, however, for the angular

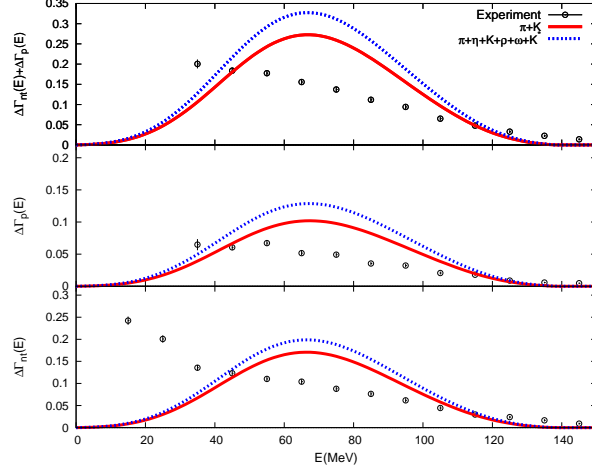


Fig. 2. Comparison between the experimental and theoretical kinetic energy spectra for neutrons (lower panel), protons (middle panel), and the sum of both (upper panel). The KEK experimental data are from [5,29], and the relation (5) has been used. The theoretical results have been evaluated from the relations  $\Delta\Gamma_p(E) = S_p(E)\Delta E$ , and  $\Delta\Gamma_{nt}(E) = [S_p(E) + 2S_n(E)]\Delta E$ , where  $\Delta E = 10$  MeV is the experimental energy bin, and  $S_N(E_N)$  are given by (19). Two OME potentials have been used: M1) only  $\pi + K$  exchange is considered, and M2) full  $\pi + K + \eta + \rho + \omega + K^*$  exchange is taken into account.

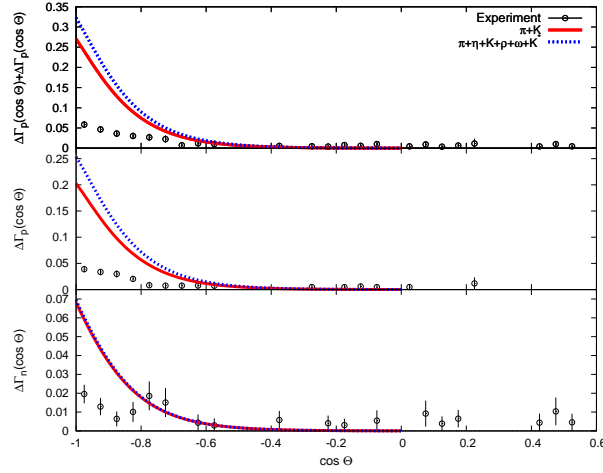


Fig. 3. Comparison between experimental and calculated opening angle correlations for neutron-neutron pairs (lower panel), proton-neutron pairs (middle panel), and the sum of both (upper panel). The KEK experimental data are from [5,29], and the relations (5) have been used. The theoretical results have been evaluated from the relations  $\Delta\Gamma_N(\cos\theta_{nN}) = S_N(\cos\theta_{nN})\Delta\cos\theta$ , where  $\Delta\cos\theta = 0.05$  is the experimental opening angle bin, and  $S_N(\cos\theta_{nN})$  are given by (20). The same OME potentials have been used as in Fig. 2.

distributions, and the c.m. momenta of the  $nN$  pairs shown in Figs. 3, and 4, where the theory overestimates the data quite significantly, and particularly for the  $np$  pairs. It could be worth noticing that both potentials yield very similar results for the  $nn$  pairs.

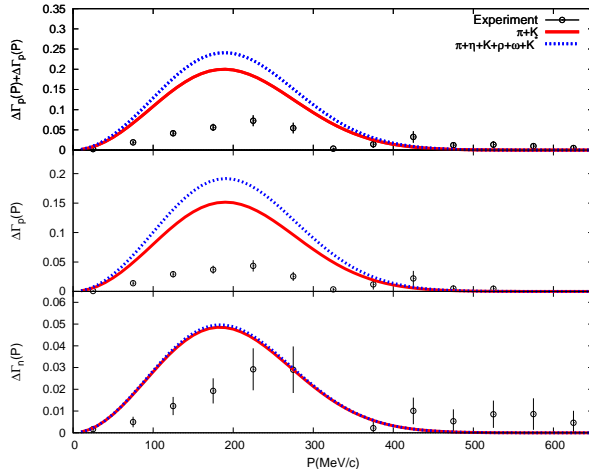


Fig. 4. Comparison between experimental and calculated c.m. momentum for neutron-neutron pairs (lower panel), proton-neutron pairs (middle panel), and the sum of both (upper panel). The KEK experimental data are from [5,29], and relations (5) have been used. The theoretical results have been evaluated from the relations  $\Delta\Gamma_N(P_{nN}) = S_N(P_{nN})\Delta P$ , where  $\Delta P = 50$  MeV/c is the experimental center of mass momentum bin, and  $S_N(P_{nN})$  are given by (23). The same OME potentials have been used as in Fig. 2.

The experimental decay rates  $\Gamma_N$  are obtained by summing over all  $\Delta\Gamma_N$  in Figs. 2, 3, and 4. The results are shown in the first three rows of Table 1. In the following two rows the results of the IPSM calculation are exhibited. No energy or angular cutoffs are done on the calculated results, since their effects are insignificant. It is self evident that the theory overestimates the data and in particular so in the case M1. We are aware that a more elaborate description of the SRCs, as performed in Ref. [13], could improve the agreement between data and theory for transition rates which are shown in Table 1. In this regard the FSIs could also help, which in addition are able to modify the spectra by redistributing the calculated transition strengths. On the other hand the new  $2N$ -NM channel can only increase the theoretical results but never decrease them, and thus the discrepancy with experiment would be still more pronounced.

The measurement of  $\Gamma_2$  in Ref. [5] is based on INC- $1N$  calculations that overestimate the data above thresholds  $E_N > 30$  MeV for both single and coincidence spectra. The authors denominate this difference as "quenching" of data in relation to theory [5,26]. Moreover, they attribute it to the lack of the  $2N$ -NM channel, which when incorporated, in proportion of  $\Gamma_2/\Gamma_{NM} = 0.29 \pm 0.13$ , decreases the calculated decay rate  $\Gamma_{NM}$  and yields agreement with data. Several observations are pertinent here:

1) Usually the word "quenching" has a different meaning in nuclear physics. The emblematic example is that of Gamow-Teller (GT) strength, the experimental value of which, either from nuclear  $\beta$ -decay or from charge-exchange reactions, is in general overestimated by calculations. This discrepancy is often resolved by including additional



Table 1

Comparison between the experimental transition rates derived from Figs. 2, 3, and 4, and the IPSM calculation, making use of two OME potentials: M1) exchange of  $\pi + K$  only, and M2) full  $\pi + K + \eta + \rho + \omega + K^*$ . The results for Fig. 2 correspond to the proton and neutron thresholds  $E_N \geq 35$  MeV.

Source	$\Gamma_p$	$\Gamma_n$	$\Gamma_p + \Gamma_n$	$\Gamma_{nt}$	$\Gamma_p + \Gamma_{nt}$
Fig. 2	$0.419 \pm 0.013$	–	–	$0.823 \pm 0.016$	$1.242 \pm 0.021$
Fig. 3	$0.197 \pm 0.024$	$0.147 \pm 0.022$	$0.345 \pm 0.033$	–	–
Fig. 4	$0.197 \pm 0.023$	$0.136 \pm 0.022$	$0.338 \pm 0.033$	–	–
M1	0.627	0.201	0.828	1.455	1.656
M2	0.792	0.205	0.997	1.789	1.994

degrees of freedom; neither the total theoretical value of the GT operator  $\sigma\tau$  is modified nor opening of new decay or reaction channels is required.

2) The present calculation also overestimates the data. Nevertheless, we do not dare to state that the NM transition operator  $V(p_{nN})$  is quenched, since as pointed out previously its evaluation involves many uncertainties, which is not the case with the GT operator.

3) The INC sequence in the calculations of the FSIs performed so far [39,40,44,45] is always triggered by the primary  $nN$  or  $nNN$  nucleons. These nucleons are produced by the same OME dynamics as we have used here. In the KEK calculation the primary NM weak dynamics is totally ignored [5].

4) The Monte Carlo study of  ${}^{12}_{\Lambda}\text{C}$  performed in Refs. [39,40], where the production of primary nucleons is described according to IPSM, does not show any evidence of the "quenching" reported in Ref. [5]. This fact suggests that the uncertainties in the FSIs calculation must be carefully considered before extracting definite conclusions from comparison of the INC results with the experimental data.

5) The above mentioned uncertainties embedded in the KEK description of the primary NM decay dynamics cannot but be augmented when the FSIs are considered. Therefore, the ambiguities involved in INC-1N calculation are probably as large or still larger than the observed "quenching".

Briefly, in our opinion the reckoning followed by the KEK group is not sufficiently robust to support the statement that the NM  $nNN$ -decay mode has been unequivocally observed experimentally.

#### 4. FINUDA Experiment

The comparison between FINUDA [6,30] experimental data and the IPSM calculation for the proton kinetic energy spectra is shown in Fig. 5. One sees that the theory overestimates the data significantly, particularly in the case of  ${}^7_{\Lambda}\text{Li}$ . Similarly as in the case of the KEK data, discrepancies between data and theory, are manifested also in the case of FINUDA transition rates  $\Gamma_p$ , as can be seen from Table 2.

The determination of the branching ratio  $\Gamma_2/\Gamma_{NM}$  in Ref. [6] is based on: i) separating the total number of detected protons  $N_p$  into low, and high energy regions populated by  $N_p^<$ , and  $N_p^>$  protons, respectively, and ii) assuming that the 1N-NM decay rates of the primary protons  $N_p^0 \equiv N(\Lambda p \rightarrow np)$  are equal in these two regions, *i.e.*,  $\Gamma_p^{0,<} = \Gamma_p^{0,>} = \Gamma_p^0/2$ , where the superscript 0 indicates that this decay rate, unlike those in Tables 1

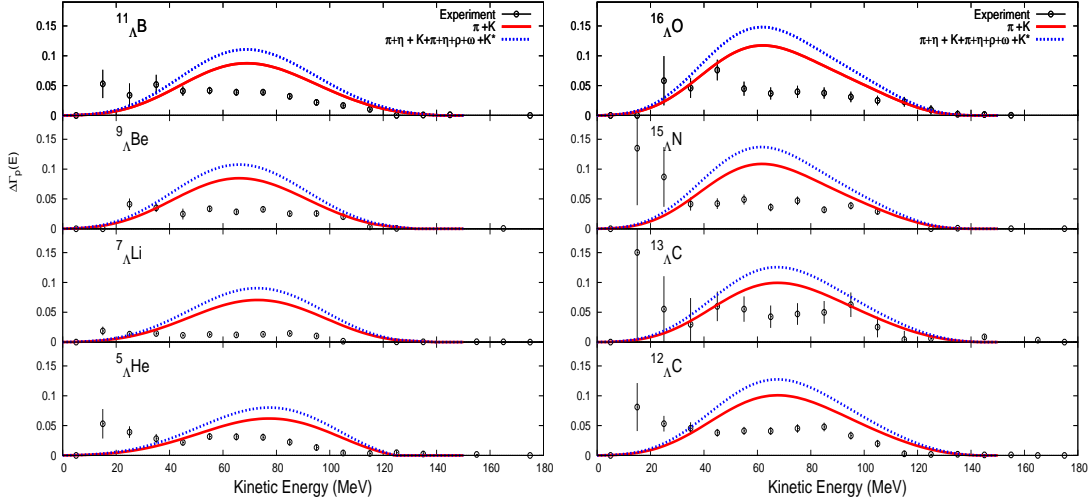


Fig. 5. Experimental data [6,30] for proton kinetic energy spectra are compared with the IPISM results. Theoretical results have been evaluated from the relation  $\Delta\Gamma_p(E) = S_p(E)\Delta E$ , where  $\Delta E = 10$  MeV is the experimental energy bin. The same OME potentials have been used as in Fig. 2.

Table 2

In the first three columns the comparison is done between the experimental transition rates  $\Gamma_p$  derived from Figs. 5 and the IPISM calculation, making use of two OMEP: M1) full  $\pi + K + \eta + \rho + \omega + K^*$ , and M2) exchange of  $\pi + K$  only. In the last two columns are listed the mean values of the Gaussian fit as obtained in Ref. [6], and calculated maxima within the IPISM, in units of MeV.

Hypernucleus	$\Gamma_p^{\text{FINUDA}}$	$\Gamma_p^{\text{M1}}$	$\Gamma_p^{\text{M2}}$	$\hat{E}^{\text{FINUDA}}$	$\hat{E}^{\text{IPSM}}$
${}^5_{\Lambda}\text{He}$	0.284	0.466	0.360	$68.5 \pm 4.1$	76.7
${}^7_{\Lambda}\text{Li}$	0.123	0.531	0.415	$76.7 \pm 5.2$	72.3
${}^9_{\Lambda}\text{Be}$	0.269	0.627	0.494	$78.2 \pm 6.2$	66.2
${}^{11}_{\Lambda}\text{B}$	0.380	0.667	0.527	$75.1 \pm 5.0$	68.9
${}^{12}_{\Lambda}\text{C}$	0.358	0.792	0.627	$80.2 \pm 2.1$	67.5
${}^{13}_{\Lambda}\text{C}$	0.437	0.776	0.614	$83.9 \pm 12.8$	67.6
${}^{15}_{\Lambda}\text{N}$	0.402	0.821	0.651	$88.1 \pm 6.2$	61.6
${}^{16}_{\Lambda}\text{O}$	0.320	0.906	0.718	$93.1 \pm 6.2$	62.0

and 2, doesn't contain contributions coming from the FSIs and  $2N$ -NM decay. Moreover, they write

$$R \equiv \frac{N_{<}}{N} = \frac{0.5 + \Gamma_2/\Gamma_p^0 + N_{<}^{\text{FSI}}/N_p^0}{1 + \Gamma_2/\Gamma_p^0 + N^{\text{FSI}}/N_p^0}, \quad (25)$$

where  $N^{\text{FSI}} = N_{<}^{\text{FSI}} + N_{>}^{\text{FSI}}$ . The partition energies  $\hat{E}$  are fixed as being the mean values of Gaussian-function fits of each proton spectrum from 80 MeV onwards, and the experimental values of the ratios  $R \equiv N_{<}^{\text{FSI}}/N_p^0$  found in this way are approximated by a linear function of the mass number  $A$ , *i.e.*,

Table 3

Results for the  $\chi^2$  parameters  $a$  and  $b$ , and the corresponding ratios  $\Gamma_2/\Gamma_p^0$ , and  $\Gamma_2/\Gamma_{NM}$ ; A) Ref. [6], B) data from Ref. [6], and the peak energies  $\hat{E}^{\text{IPSM}}$  from last column in Table 2 instead of  $\hat{E}^{\text{FINUDA}}$ , and C) same as in B but performing the fit with Eq. (30) instead of Eq. (26).

case	$a$	$b$	$\Gamma_2/\Gamma_p^0$	$\Gamma_2/\Gamma_{NM}$
A	$0.654 \pm 0.138$	$0.009 \pm 0.013$	$0.43 \pm 0.25$	$0.24 \pm 0.10$
B	$0.674 \pm 0.108$	$-0.008 \pm 0.009$	$0.53 \pm 0.51$	$0.26 \pm 0.10$
C	$0.135 \pm 0.408$	$0.207 \pm 0.202$	$-0.42 \pm 0.14$	$-0.40 \pm 0.10$

$$R(A) = a + bA, \quad \text{where} \quad a = \frac{0.5 + \Gamma_2/\Gamma_p^0}{1 + \Gamma_2/\Gamma_p^0}, \quad (26)$$

does not depend on  $A$ , and yields

$$\frac{\Gamma_2}{\Gamma_p^0} = \frac{a - 0.5}{1 - a}, \quad \frac{\Gamma_2}{\Gamma_{NM}} = \frac{a - 0.5}{(1 - a)\Gamma_n^0/\Gamma_p^0 + 0.5}. \quad (27)$$

Finally, a  $\chi^2$  fit for  $R(A)$  was done obtaining the values of  $a$ , and  $b$  shown in the row A of Table 3, together with the resulting  $\Gamma_2/\Gamma_p^0$ , and  $\Gamma_2/\Gamma_{NM}$  derived from (27) with  $\Gamma_n^0/\Gamma_p^0 = 0.48 \pm 0.08$ , which is the mean value of recent experimental results [26].

The manner of deducing the 2N-NM decay rate as performed in Ref. [6] can be challenged from several aspects which we point out below.

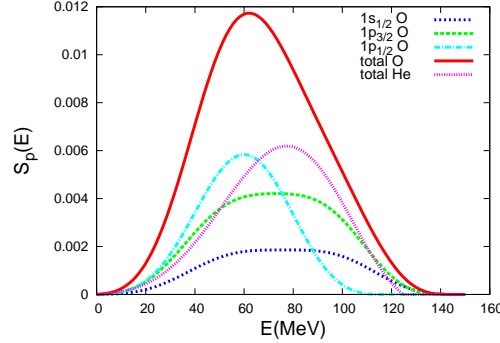


Fig. 6. Calculated  ${}^5\text{He}$  and  ${}^{16}\text{O}$  spectra within the IPSM employing the  $\pi + K$  transition potential. Contributions of different partial waves  $s_{1/2}$ ,  $p_{3/2}$ , and  $p_{1/2}$  to the total  ${}^{16}\text{O}$  spectra are also displayed.

1) How to arrive from (25) to (26) is not a trivial issue. One possibility is to neglect the last term in the denominator of (25), arguing, as was done in Ref. [6], that the FSIs tend to remove protons from the high energy part of the spectrum ( $N_{>}^{FSI} < 0$ ) while filling the low energy region ( $N_{<}^{FSI} > 0$ ), with the net result that  $N^{FSI} = N_{<}^{FSI} + N_{>}^{FSI} \cong 0$ . Therefore

$$R \cong a + \frac{N_{<}^{FSI}}{(1 + \Gamma_2/\Gamma_p^0)N_p^0} \cong a + \frac{N_{<}^{FSI}}{N_p^0}, \quad (28)$$

which, when compared with (26), yields

$$N_{<}^{FSI} \cong bAN_p^0. \quad (29)$$

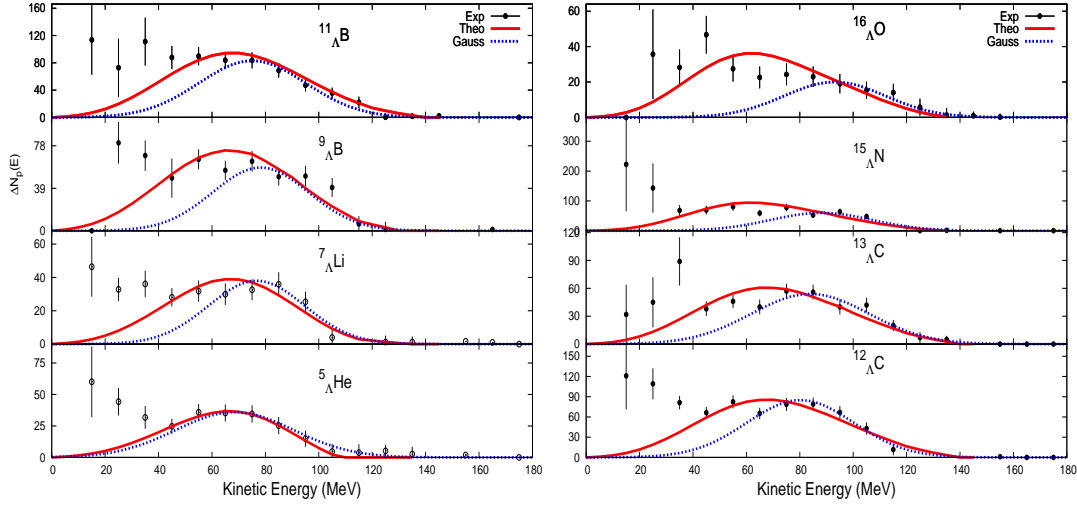


Fig. 7. Experimental data and Gaussian fits from Ref [6] for proton kinetic energy spectra, are compared with the IPISM results normalized for proton energy  $E_p \geq 40$  MeV.

At first glance this sounds reasonable because the effect of FSIs should increase with  $A$ . But, since  $b = 0.009 \pm 0.013$  one finds that the number of particles  $N_{<}^{FSI}$  per nucleon that are dislocated from high to low energy is less than 1% of the total number of primary protons produced by the  $1N$ -NM decay, which is unrealistic.

2) The assumption  $\Gamma_p^{0<} = \Gamma_p^{0>} = \Gamma_p^0/2$  is badly supported by the IPISM, where  $\Gamma_p^{0>}$  becomes progressively larger than  $\Gamma_p^{0<}$  as the mass number is increased. Why it is so can be understood from inspection of Fig. 6, where the spectra of  ${}^5_{\Lambda}\text{He}$  and  ${}^{16}_{\Lambda}\text{O}$  are displayed. In the case of  ${}^5_{\Lambda}\text{He}$  only the orbital  $s_{1/2}$  contributes, being  $\Gamma_p^{0<}$  appreciably larger than  $\Gamma_p^{0>}$  ( $\Gamma_p^{0<} = 0.55\Gamma_p^0$ ), for other hypernuclei also the orbitals  $p_{3/2}$ , and  $p_{1/2}$  contribute. Their spectra are wider and localized at higher energies than the corresponding  $s_{1/2}$  strength. This causes the total transition strength to be gradually shifted towards higher energies as  $A$  increases, becoming  $\Gamma_p^{0<} = 0.43\Gamma_p^0$  for  ${}^{16}_{\Lambda}\text{O}$ .

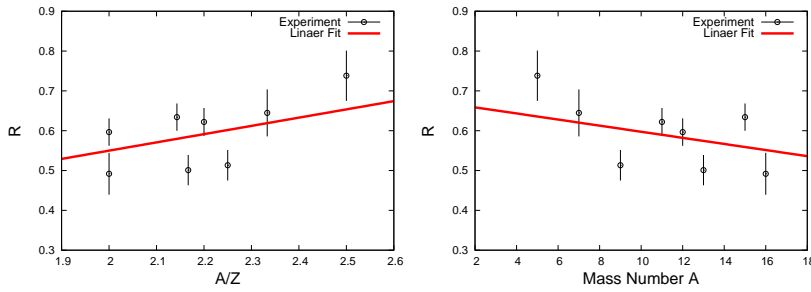


Fig. 8. Ratio  $R$  as a function of  $A$  (left panel), and of  $A/Z$  (right panel). In both cases the energies  $\hat{E}^{\text{IPISM}}$ , and the corresponding  $R \equiv N_{<}/N$  are used.

3) Except for  ${}^5_{\Lambda}\text{He}$ , the calculated proton spectra deviate significantly from the Gaussian fits adopted in Ref. [6] for the  $1N$ -NM decay. Although bell shaped they differ both

in energies  $\hat{E}$  and in FWHM widths. This can be observed from Table 2, and Fig. 7, where the IPSM results are normalized to the experimental data for proton energies  $E_p \geq 40$  MeV. Both OMEP models yield the same normalized spectra, since the spectrum shapes depend only on kinematics.

4) Large differences between  $\hat{E}^{\text{FINUDA}}$ , and  $\hat{E}^{\text{IPSM}}$ , shown in Table 2, give rise to large differences between values of ratio  $R$  in Ref. [6, Fig. 2], and our values exhibited in Fig. 8. On the left and right panels of this figure are shown the linear  $\chi^2$  fits of  $R$  given by (26), and by

$$R(A, Z) = a + bA/Z, \quad (30)$$

respectively. The later is also a possible parametrization for (25), as suggested by expression (28) since  $N_p^0$  should be proportional to the number of protons  $Z$  [38]. The resulting values of  $a$ ,  $b$ ,  $\Gamma_2/\Gamma_p^0$ , and  $\Gamma_2/\Gamma_{\text{NM}}$  are listed listed in rows B and C of Table 3. One sees that  $a$ , and therefore  $\Gamma_2/\Gamma_p^0$ , and  $\Gamma_2/\Gamma_{\text{NM}}$  are very similar in cases A and B. However, the value of parameter  $b$  is negative in case B, which makes its physical interpretation still more embarrassing than in case A, since from (29) it follows that the number  $N_{<}^{\text{FSI}}$  becomes negative, and therefore the FSIs now move particles from low to high energy. Finally, in case C the ratios  $\Gamma_2/\Gamma_p^0$ , and  $\Gamma_2/\Gamma_{\text{NM}}$  turn out to be large and negative, which obviously doesn't make sense.

We conclude therefore, that similarly to the KEK experiment [5], the argumentation followed by the FINUDA group [6] can yield several quite different results for the ratio  $\Gamma_2/\Gamma_{\text{NM}}$ .

## 5. Summary and Conclusions

We have discussed the new KEK [5] and the FINUDA [6] experiments on the non-mesonic weak decay of hypernuclei in the framework of the IPSM, with the dynamics described by the OPE mechanism, and using two different models: M1) with  $\pi+K$  mesons only, and M2) that comprises the exchange of the complete pseudoscalar and vector meson octets ( $\pi, \eta, K, \rho, \omega, K^*$ ). We prefer the first one since the coupling constants  $NN\pi$ , and  $N\Lambda\pi$  are well established, and the only parameters that are still uncertain in this case are the coupling strengths  $NNK$ , and  $N\Lambda K$ . Of course, except for reasons of simplicity, there is no justification for not including the remaining mesons.

We found that the theory overestimates the data to a great extent. There could be several reasons for this, such as: i) the absence of the FSIs in the employed model, ii) the uncertainties inherent in the OME model, iii) the approximation used for the SRCs, *etc.*

We argue that at present there exist many uncertainties, on both sides experimental and theoretical, which prevent us to draw definite conclusions regarding the  $2N$ -NM decay rate  $\Gamma_2$ . In view of this situation we are developing the IPSM formalism for this decay channel [46] that will be confronted with the FGM, which is the only approach used so far [9]. Once this is accomplished it will also enable us to study the effects of FSIs on the three-nucleon emission. New developments in this field of experimentation will be very welcome. Needless to say that triple  $(p, n, n)$ , and  $(p, p, n)$  coincidence measurements will be extremely useful for direct measurement of  $\Gamma_2$ .

After completing the present work we have learnt that a new derivation of the ratio  $\Gamma_2/\Gamma_{\text{NM}}$  has been done at FINUDA, based on the analysis of the  $(\pi^-, p, n)$  triple coincidence events [47]. The result is similar to the previous one [6].

### ACKNOWLEDGEMENTS

FK is supported by the Argentinean agency CONICET under contract PIP 0377. AD is supported by the Brazilian agencies FAPESP and CNPQ. We are grateful to Eduardo Bauer, Joe Parker, and Gianni Garbarino for helpful discussion and critical reading of the manuscript. We also wish to express our sincere thanks to Gordana Tadić for the meticulous review of the manuscript.

### References

- [1] W.M. Alberico, G. Garbarino, Phys. Rep. **369** 1 (2002)
- [2] J. Schneps, W.F. Fry, and M.S. Swami, Phys. Rev. **106**, 1062 (1957).
- [3] W.M. Alberico, A. De Pace, M. Ericson, and A. Molinar, Phys. Lett. **B 256** (1991) 134.
- [4] A. Ramos, E. Oset and L.L. Salcedo, Phys. Rev. **C 50**, 2314 (1994).
- [5] M.J. Kim, *et al.*, Phys. Rev. Lett. **103**, 182502 (2009).
- [6] M. Agnello *et al.*, Phys. Lett. **B 685** (2010) 247.
- [7] E. Bauer, and G. Garbarino, Nucl. Phys. **A 828** 29 (2009).
- [8] J. D. Parker *et al.*, Phys. Rev. **C 76** (2007) 035501.
- [9] E. Bauer, A.P. Galeão, M. Hussein, F. Krmpotić, and J.D. Parker, Phys. Lett. **B 674**, 103 (2009).
- [10] E. Bauer, and G. Garbarino, Phys. Lett. **B 698** 306 (2011).
- [11] V. G. J. Stoks, R. A. M. Klomp, C. P. F. Terheggen, and J. J. de Swart, Phys. Rev. **C 49** (1994)(2003) 2950.
- [12] A. Parreño, A. Ramos, and C. Bennhold, Phys. Rev. **C 56**, 339 (1997).
- [13] A. Parreño, A. Ramos, Phys. Rev. **C 65**, 015204 (2002).
- [14] K. Sasaki, T. Inoue, and M. Oka, Nucl.Phys. **A 669**, 331 (2000); Erratum-ibid. **A678**, 455 (2000).
- [15] K. Sasaki, T. Inoue, and M. Oka, Nucl. Phys. **A 707**, 477 (2002).
- [16] A. Parreño, C Bennhold, and B. R. Holstein, Phys. Rev. **C 70**, 051601 (2004).
- [17] C. Chumillas, G. Garbarino, A. Parreño, and A. Ramos, Phys. Lett. **B657**, 180 (2007).
- [18] K. Itonaga, T. Motoba, T. Ueda, and Th.A. Rijken, Phys. Rev. **C 77**, 044605 (2008).
- [19] A. Ramos, M. J. Vicente-Vacas, and E. Oset, Phys. Rev. **C 55**, 735 (1997); Phys. Rev. **C 66**, 039903 (2002)(E).
- [20] J.H. Kim *et al.*, Phys. Rev. **C 68** (2003) 065201.
- [21] S. Okada *et al.*, Phys. Lett. **B 597** (2004) 249.
- [22] S. Okada *et al.*, Nucl. Phys. **A 752** (2005) 169c.
- [23] H. Outa *et al.*, Nucl. Phys. **A 754** (2005) 157c.
- [24] B.H. Kang *et al.*, Phys. Rev. Lett. **96**, 025203 (2006).
- [25] M.J. Kim *et al.*, Phys. Lett. **B 641**, 28 (2006).
- [26] H. Bhang *et al.*, Eur. Phys. J. **A 33** (2007) 259.
- [27] M. Agnello *et al.*, Nucl. Phys. **A 804** (2008) 151.
- [28] M. Agnello *et al.*, Phys. Lett. **B 681** (2009) 139.
- [29] H. Bhang, private communication.
- [30] G. Garbarino, private communication
- [31] C. Barbero, D. Horvat, F. Krmpotić, T. T. S. Kuo, Z. Narančić, and D. Tadić, Phys. Rev. **C 66**, 055209 (2002).
- [32] F. Krmpotić, and D. Tadić, Braz. J. Phys. **33**, 187 (2003).
- [33] C. Barbero, C. De Conti, A. P. Galeão and F. Krmpotić, Nucl. Phys. **A 726**, 267 (2003).
- [34] C. Barbero, A. P. Galeão, and F. Krmpotić, Phys. Rev. **C 76**, 0543213 (2007).
- [35] C. Barbero, A. P. Galeão, M. Hussein, and F. Krmpotić, Phys. Rev. **C 78**, 044312 (2008); Erratum-ibid. 059901(E).
- [36] E. Bauer, A. P. Galeão, M. S. Hussein and F. Krmpotić, Nucl. Phys. **A 834** 599c (2010).
- [37] F. Krmpotić, A. P. Galeão, and M.S. Hussein, *AIP Conf. Proc.* **1245**, 51 (2010).

- [38] F. Krmpotić, Phys. Rev. **C 82**, 05520 (2010).
- [39] I. Gonzalez *et al.*, J. Phys. Conf. Ser. 312, 022017 (2011)
- [40] I. Gonzalez, C. Barbero, A. Deppman, S. Duarte, F. Krmpotić, O. Rodriguez, J. Phys. G: Nucl. Part. Phys. 38 (2011) 115105.
- [41] M. Rho *et al.*, Nucl. Phys. **A 231** (1974) 493.
- [42] K. Nakayama, A. P. Galeão, and F. Krmpotić, Phys. Lett. **B114**, 217 (1982).
- [43] F. Osterfeld, Rev. Mod. Phys. **64**, 491 (1992), and references therein.
- [44] G. Garbarino, A. Parreno and A. Ramos, Phys. Rev. Lett. 91 (2003) 112501; Phys. Rev. C 69 (2004) 054603.
- [45] E. Bauer, G. Garbarino, A. Parreño, and A. Ramos, Nucl. Phys. **A 836**, 199 (2010).
- [46] C. Barbero, E. Bauer, C. De Conti, A. P. Galeão and F. Krmpotić, in preparation.
- [47] M. Agnello *et al.*, Phys. Lett. **B 701** (2011) 556.